NANO LETTERS

2001
Vol. 1, No. 11
605−611

Energy Levels in Embedded Semiconductor Nanoparticles and Nanowires

Karuna K. Nanda,* F. Einar Kruis, and Heinz Fissan

Department of Electrical Engineering and Information Technology, Faculty of Engineering Sciences, Gerhard-Mercator-University, Bismarckstr. 81, 47057 Duisburg, Germany

Received May 3, 2001; *Revised Manuscript Received August 15, 2001*

ABSTRACT

A finite-depth square-well model is used to show that the band gap of a nanoparticle for a given size can be tuned by embedding the nanoparticle in different matrices. This may find a technological importance in different branches of physics. The band gaps calculated using this model are found to be consistent with reported experimental band gaps of semiconductor materials (PbS and CdS) embedded in different matrices. A new wave function for a one-dimensional semiconductor has been deduced to evaluate the size-dependent band gap of a semiconductor wire, explaining the variation of the band gap of porous Si with the ratio of Si–O and Si–H bond concentrations.

It is well known that the band gap of a semiconductor nanoparticle increases as the particle size decreases. However, the reported experimental band gaps of different semiconductors are inconsistent. For example, Wang et al.[1] have observed a band gap of ∼2.4 eV for PbS nanoparticles of diameter ∼1.0 nm capped with ethylene-15% methacrylic acid copolymer (E-MAA), whereas the band gap is 5.2 eV for 1.0 nm diameter PbS particles embedded in dielectric SiO_2 matrix.[2] Similarly, for polymer capped 1.0 nm diameter CdS particles the band gap is 3.53 eV,[3] whereas for ∼1.3 nm CdS particles stabilized in 1-thioglycerol[4] the band gap is 4.78 eV, and for 2.4 nm CdS particles embedded in silicate glass the band gap is 3.5 eV.[5] Furthermore, it has been shown for porous silicon that the photoluminescence (PL) peak energy depends on the surface conditions of the porous silicon. The PL peak energy is found to increase almost logarithmically with the ratio of Si−O/Si−H bond concentration.[6] Very recently, Passseo et al.[7] have also shown that the wavelength of luminescence of InGaAs quantum dots can be tuned by controlling the barrier embedding quantum dots. One of the possible explanations for this discrepancy in the reported value of the band gap might be due to the influence of the surrounding matrix and the surface conditions. If this is the case, it is possible to tune the band gap of semiconducting nanoparticles of a given size by changing the surrounding matrix and surface conditions.

The tuning of the band gap of a semiconductor system for a given particle size may find a technological importance in different branches of physics. One example is in photoelectrochemical cells (PECs). To be practically useful as a PECs material, a semiconductor should have a band gap small enough to absorb an appreciable portion of the solar spectrum in order to produce a large current. On the other hand the semiconductor material must have a band gap large enough so that the open-circuit current should be small. These considerations limit materials for photovoltaic applications to those with a band gap in the 1.0−2.0 eV range.[8] Further, the loss of quantum efficiency in PECs is due to electron−hole recombination in the bulk and at the surface of the semiconductor. The bulk recombination can be controlled by reducing the size of the nanoparticles,[9] whereas the surface recombination can be decreased by passivating the nanoparticle surface. In this context, it is important to note that the efficiency of PECs and that of an electroluminescence device can be improved by embedding n-type nanoparticles within a p-type semiconducting polymer or by embedding p-type nanoparticles within an n-type semiconducting polymer.[10,11] The above discussion reveals that the particle size should be as small as possible with the band gap in the 1.0−2.0 eV range for the use in PECs. Another important technological direction is the use of nanometer-sized semiconductor particles as potential amplifiers operating at 1.3 and 1.5 μm wavelengths for telecommunication devices, which for a given material can be achieved by changing the particle size. Chemical methods of nanoparticle synthesis do usually not allow to obtain monocrystalline particles over a wide size range.[12,13] It would be useful for practical application if it is possible to control the band gap of a semiconductor nanoparticle for a given size.

* E-mail: nanda@uni-duisburg.de; Phone: +49 (0) 203 379 3909; Fax: +49 (0) 203 379 3268

10.1021/nl0100318 CCC: $20.00
Published on Web 09/20/2001

Different models have been proposed to understand the blue shift of the band gap as a function of particle size. Wang et al.[1] proposed a hyperbolic band model to include the band nonparabolicity and derived an expression for the band gap that explains the observed size-dependence of the band gap of PbS nanoparticles down to 2.5 nm. However, this model cannot account for the difference in the band gap of a nanoparticle when embedded in different matrices or when the surface condition is changed. Many researchers[14−21] have considered the square-well potential to understand the size-dependent optical properties of low-dimensional semiconducting systems because of its simplicity. In treating low-dimensional systems, three categories are usually considered: the so-called two-dimensional (2D) systems, which include thin films, layer structures, quantum wells and superlattices; the one-dimensional (1D) systems, such as semiconductor wires; and zero-dimensional (0D) systems, such as clusters, quantum dots, and colloids. In 2D and 0D semiconductors, the exact ground-state wave function can be used for the evaluation of the different physical properties, whereas the wave function in 1D is approximated[22] for the same. In this letter, a *new* wave function for 1D semiconductors is derived, which is a better approximation to the exact one[22] and also suitable for the calculation of different physical properties.[22,23] The size-dependent band gap is evaluated using the ground-state wave functions and the physical values of the barrier height and then compared with different experimental results on the size-dependent band gap of different semiconductors, as published in the literature. Interestingly, this model explains *quantitatively* the size dependence of the band gap of a semiconducting material embedded in different matrices and sets a limit to the possible extreme values of the band gap.

Finite-Depth Square-Well Model. It is well established that the effective mass approximation overestimates the band gap of very small particles where it is assumed that the carriers are confined within a spherical well of infinite depth ($V_0 \rightarrow \infty$).[1,24] Further, the square-well potential assumption with infinite depth cannot account for the influence of the surrounding matrix on the band gap of a semiconductor nanoparticle. When a semiconductor material is embedded within another semiconducting matrix having a higher band gap, V_0 is defined as

$$E_g^{(m)} = E_g^{(s)} + V_{0e} + V_{0h} \tag{1}$$

where $E_g^{(s)}$ and $E_g^{(m)}$ are the band gap energies of the semiconductor material and the matrix, respectively. V_{0e} and V_{0h} are the confined potentials of electrons and holes, respectively (Figure 1). Further, the mass of the electrons or holes is considered to be the effective mass m^* inside the semiconductor and the free mass m_0 outside the semiconductor.[21] In the boundary condition at the surface, the derivatives of the functions are divided by the mass.[15,18] To evaluate the size-dependent band gap of low-dimensional semiconductors, we concentrate only on the ground state energy eigen values.

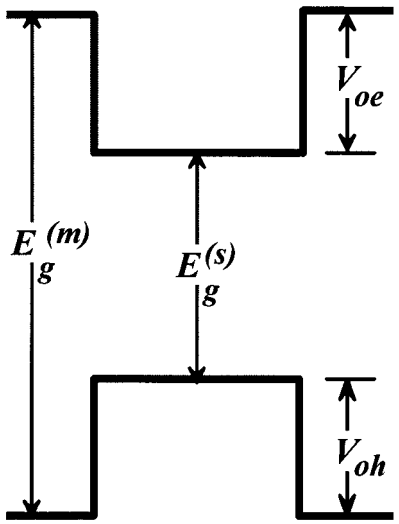

Figure 1. Potentials (V_{0e} and V_{0h}) for a semiconductor material in a matrix. The depth of the potentials (V_{0e} and V_{0h}) depends on the surrounding matrix.

1D Semiconductors. The radial Schrödinger equations for a 1D semiconductor are

$$\frac{d^2\Phi}{d\rho^2} + \frac{1}{\rho}\frac{d\Phi}{d\rho} + \beta^2\Phi = 0, \quad \rho < a \tag{2a}$$

and

$$\frac{d^2\Phi}{d\rho^2} + \frac{1}{\rho}\frac{d\Phi}{d\rho} - \alpha^2\Phi = 0, \quad \rho > a \tag{2b}$$

with

$$\frac{2m_0E}{\hbar^2} = -\alpha^2 \quad \text{and} \quad \frac{2m^*(E+V_0)}{\hbar^2} = \beta^2; \quad \alpha, \beta > 0 \tag{3}$$

so that

$$m^*\alpha^2a^2 + m_0\beta^2a^2 = \frac{2m_0m^*V_0a^2}{\hbar^2} = \frac{m_0V_0}{\Delta} \tag{4}$$

where

$$\Delta = \frac{\hbar^2}{2m^*a^2}$$

and where a is the range of the potential. The ground-state solutions of eqs 2a and 2b are

$$\Phi = CJ_0(\beta\rho),\ \rho < a \quad \text{and} \quad \Phi = DK_0(\alpha\rho),\ \rho > a \tag{5}$$

respectively. C and D are normalization constants, $J_0(z)$ is the Bessel function of the first kind and $K_0(z)$ is the Bessel

function of the second kind, which decreases exponentially with increasing z. The exact ground-state wave function for $\rho < a$ is[22]

$$\Phi(\rho < a) = \frac{1}{\sqrt{\pi}a}\frac{1}{J_1(\beta)}J_0(\beta\rho/a) \tag{6}$$

For an infinite potential the wave function vanishes at $\rho = a$, which implies that the solution of eq 6 is given by $\beta = \beta_0 \approx 2.4$. The integral representation of $J_0(z)$ is[25]

$$J_0(z) = \frac{1}{\pi}\int_0^{\pi} \cos(z\sin\theta)\, d\theta$$

When the argument z is much smaller than unity, $J_0(z)$ can be approximated as

$$J_0(z) \cong \cos(z/\sqrt{2})$$

Thus, the ground state wave function for $\rho < a$ can be written as

$$\Phi(\rho < a) \cong A\cos(\beta\rho/\sqrt{2}) \tag{7}$$

Based on eq 7, we can write the normalized wave function as

$$\Phi(\rho < a) = \sqrt{\frac{3.363}{\pi a^2}}\cos\frac{\pi\rho}{2a} \tag{8}$$

At the boundary of the semiconductor, the wave function corresponding to a infinite potential vanishes, which implies that $\beta a/\sqrt{2} = \pi/2$. To obtain an analytical result for electron−electron and electron−impurity interactions, Gold and Ghazali[22] have used the following expression of the normalized wave function in the infinite barrier height approximation:

$$\Phi(\rho < a) = \sqrt{\frac{3}{\pi a^2}}\left(1 - \frac{\rho^2}{a^2}\right) \tag{9}$$

The wave functions according to eqs 6, 8, and 9 are compared in Figure 2. It can be noted from the figure that the analytical expression, given in eq 8, is a better approximation to the exact one than is that of ref 22. To test the approximation (eq 8) further, we estimate the energy eigen value, which is given by

$$E_0(1\mathrm{D}) + V_0(\rightarrow\infty) = \frac{\hbar^2\pi^2}{4m^*a^2} \approx 4.935\frac{\hbar^2}{2m^*a^2} \tag{10}$$

and is similar to the exact expression for the energy eigen value with a prefactor of 5.76 instead of 4.935.[22] To get a prefactor of 5.76, we modify the wave function as

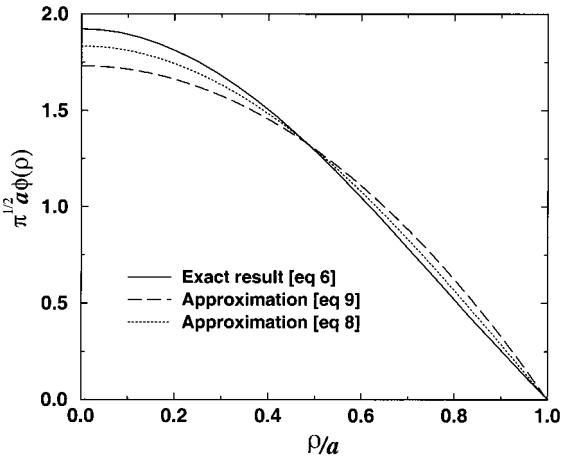

Figure 2. Comparison of the exact wave function of 1D semiconductors with the approximated ground-state wave function for an infinite potential barrier.

$$\Phi(\rho < a) \cong \sqrt{\frac{3.363}{\pi a^2}}\cos\frac{\beta\rho}{\sqrt{2.334}} \tag{11a}$$

This wave function can now be used for the evaluation of energy levels, electron−electron interactions, and electron−impurity interactions of a 1D system. Now, we discuss the wave function outside the 1D semiconductor. For $\alpha\rho \ll 1$, the Bessel function $K_0(\alpha\rho)$ can be approximated as

$$K_0(\alpha\rho) \cong -[\ln(\alpha\rho/2) + \gamma] \tag{11b}$$

where γ is the Euler constant. This leads to a negative value for the wave function for large ρ. Therefore, we use the following form of the wave function for $\rho > a$:

$$\Phi(\rho > a) \cong B\exp(-\alpha\rho) \tag{11c}$$

or

$$\Phi(\rho > a) = B^*\frac{\exp(-\alpha\rho)}{\alpha\rho} \tag{11d}$$

where B and B^* are constants. These forms of the wave function are more appropriate as $\Phi \cong 0$ for large ρ.

Applying the boundary conditions to eqs 11a and 11c, the following approximation for the eigen value equation is obtained:

$$\frac{\beta a}{\sqrt{2.334}}\tan\frac{\beta a}{\sqrt{2.334}} \cong \left(\frac{m^*}{m_0}\right)\alpha a = \sqrt{\frac{m^*}{m_0}\left(\frac{V_0}{\Delta} - \beta^2 a^2\right)} \tag{12a}$$

If the wave function in eq 11d is considered instead of that in 11c, the eigen value equation becomes

$$\frac{\beta a}{\sqrt{2.334}}\tan\frac{\beta a}{\sqrt{2.334}} \cong \left(\frac{m^*}{m_0}\right)(1+\alpha a) = \left(\frac{m^*}{m_0}\right) + \sqrt{\frac{m^*}{m_0}\left(\frac{V_0}{\Delta} - \beta^2 a^2\right)} \quad (12b)$$

When the depth of the potential is finite, there is no analytical solution for the energy eigen values. Solving eq 12 numerically, it is noted that the solution βa is a fraction of $\sqrt{2.334}\pi/2$, which depends on the value of (V_0/Δ) and m_0, i.e., $\beta a = \eta_{1D,0}\sqrt{2.334}\pi/2$, where $\eta_{1D,0}$ is a dimensionless parameter depending on V_0, m^*, m_0, and a. For a large value of the potential ($V_0 \rightarrow \infty$), $\eta_{1D,0} \rightarrow 1$ and is less than unity for smaller values of V_0 and a. Based on the above discussion, the energy eigen value can now be written as

$$E_0(1\mathrm{D}) + V_0 = \frac{2.334\hbar^2\pi^2}{8m^*a^2}\eta_{1D,0}^2 \quad (13)$$

To choose the correct wave function outside the square-well, we compared β^2a^2, estimated using eqs 12a and 12b, and found that the wave function (11c) for $\rho > a$ is more appropriate although the values of β^2a^2 for both the wave functions are comparable.

0D Semiconductors. The radial Schrödinger equations for a 0D semiconductor are

$$\frac{d^2\Phi}{d\rho^2} + \frac{2}{\rho}\frac{d\Phi}{d\rho} + \beta^2\Phi = 0, \quad \rho < a \quad (14a)$$

and

$$\frac{d^2\Phi}{d\rho^2} + \frac{2}{\rho}\frac{d\Phi}{d\rho} - \alpha^2\Phi = 0, \quad \rho > a \quad (14b)$$

The ground-state solutions of eqs 14a and 14b are

$$\Phi = Cj_0(\beta\rho), \quad \rho < a$$

and

$$\Phi = Dh_0^{(1)}(i\alpha\rho), \quad \rho > a \quad (15)$$

respectively. C and D are normalization constants, j_0 is the spherical Bessel function of first kind, and $h_0^{(1)}$ is the spherical Bessel function of third kind:

$$j_0(\beta\rho) \cong \frac{\sin\beta\rho}{\beta\rho} \quad (16a)$$

and

$$h_0^{(1)}(i\alpha\rho) = -\frac{\exp(-\alpha\rho)}{\alpha\rho} \quad (16b)$$

Applying the boundary conditions to eqs 16a and 16b, we obtain the following approximation for the eigen value equation

$$\beta a\cot\beta a = -\left(\frac{m^*}{m_0}\right)(\alpha a + 1) + 1 = 1 - \left(\frac{m^*}{m_0}\right) - \sqrt{\left(\frac{m^*}{m_0}\right)\left(\frac{V_0}{\Delta} - \beta^2 a^2\right)} \quad (17)$$

It is straightforward to see that the solution βa depends on the value of (V_0/Δ) and is a fraction of π, i.e., $\beta a = \eta_{0D,0}(V_0/\Delta)\pi$, where $\eta_{0D,0}(V_0/\Delta)$ is a function of V_0, m_0, m^*, and a. For an infinite square-well potential ($V_0 \rightarrow \infty$), $\eta_{0D,0} \rightarrow 1$ and is less than unity for smaller values of V_0 and a. The expression for the energy eigen values in 0D is

$$E_0(0\mathrm{D}) + V_0 = \frac{\hbar^2\pi^2}{2m^*a^2}\eta_{0D,0}^2(V_0, m^*, m_0, a) \quad (18)$$

To estimate the value of η^2 for 1D and 0D semiconductors, eqs 12b and 17, respectively, are to be solved numerically.

Coulomb Energy. Energy (ΔE_{e-h}) for the Coulomb interaction between an electron and a hole in a semiconductor is evaluated by

$$\Delta E_{e-h} \cong -\frac{2e^2}{\epsilon}\int_0^a \Phi^2(r_h) r_h\, dr_h\left[\int_0^{r_h} \Phi^2(r_e) r_e^2\, dr_e\right] = -\frac{16\pi^2e^2A_e^2A_h^2}{\epsilon}\left[\int_0^a \sin^2(\beta_h r_h)\, dr_h - \frac{1}{2}\int_0^a \sin^2(\beta_h r_h)\sin(2\beta_e r_h)\, dr_h/r_h\right] \quad (19)$$

in 0D. Using the wave function for the infinite-depth potential, ΔE_{e-h} in 0D is found to be

$$\Delta E_{e-h} = -1.75e^2/\epsilon a \quad (20)$$

which is in good agreement with that obtained by Brus.[26] For finite value of the potential, ΔE_{e-h} is estimated numerically and is compared with that for infinite barrier height as shown in Figure 3. It can be noted that the Coulomb energy decreases as the barrier height decreases and is in agreement with other reports.[18−20] A pseudopotential calculation[27] also suggests that the contribution of Coulomb energy is smaller as compared to eq 20. Further, as the particle size decreases the Coulomb energy first increases and then decreases. The increase in the Coulomb energy is associated with the confinement of both electron and hole as the particle size decreases. However, as the particle size is decreased further, the probability of finding an electron outside the barrier increases, and as a result of it the Coulomb energy decreases. Báyani et al.[28] have shown that the surface polarization also influences the Coulomb energy and that the effect is prominent when the dielectric constants of the surrounding matrix are substantially different. However, they assumed

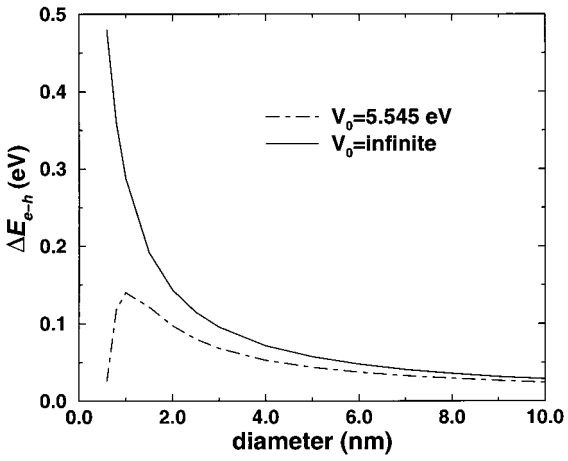

Figure 3. Coulomb energies (ΔE_{e-h}) calculated for finite-depth potential ($V_0 = 5.545$ eV) for PbS nanoparticles embedded in SiO_2. The dielectric constant of PbS is taken as $\epsilon = 17.2$.[1] The energy calculated for the infinite potential is shown by the solid line.

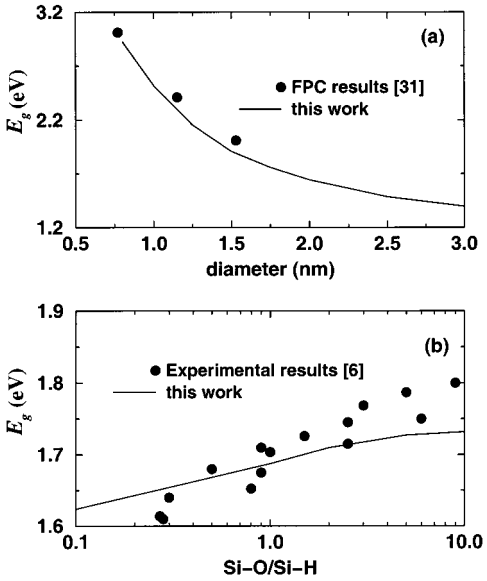

Figure 4. (a) Comparison of the band gap calculated by FPC[32] and this work for Si wire terminated by hydrogen. The parameters used are $E_g^{(m)}$(polysilane) = 4.69 eV,[31] $m_e^* = 0.2m_e$, $m_h^* = 0.5m_e$, and $m_0 = m_e$.[33] (b) Correlation between the band gap of porous silicon with the Si−O/Si−H bond concentrations. The diameter of the porous silicon is taken to 2.5 nm as it is not quoted in ref 6. The other parameters are the same as for (a).

the same effective mass inside and outside the particles, which may influence the results quantitatively. Further, it has been shown[29] that the electronic structure of CdSe nanocrystals is influenced by a polar environment, whereas nanocrystals of GaP, CdS, PbS, Si with crystal structure of higher symmetry group are expected to interact weekly with their environment. It may also be noted for CdSe that the change of the energy shifts due to the dielectric environment decreases as the dielectric constant increases [Figure 10 of ref 29]. This implies that a difference in the band gap of 2.8 eV for a 1.0 nm PbS particles embedded in SiO_2 and E-MAA cannot be accounted for by the polarization effect.

Results and Discussions. Using eq 19, we can estimate the shift in the conduction and valence band by substituting $m^* = m_e^*$ and $m^* = m_h^*$, respectively. As the change in band gap (ΔE_g) of a semiconductor particle is the sum of the shift in the conduction band and valence band, we have

$$\Delta E_g = \frac{\hbar^2\pi^2}{2a^2}\left[\frac{\eta_e^2}{m_e^*} + \frac{\eta_h^2}{m_h^*}\right] + \Delta E_{e-h} \qquad (21)$$

where m_e^* and m_h^* are the effective mass of electron and hole, respectively. To test the validity of the formulation, we compare our results with the reported experimental band gap of three different systems: (1) porous Si with different surface conditions; (2) PbS nanoparticles embedded within SiO_2 and E-MAA; and (3) CdS nanoparticles embedded within silicate glass.

(1) Porous Si with Different Surface Conditions. First, the model proposed in this work was compared with the results of first-principle calculations (FPC) for a Si quantum wire terminated by hydrogen (polysilane). As the band gap of bulk Si is 1.12 eV and that of polysilane is 4.69 eV,[30] a barrier height of 1.785 eV is obtained for Si terminated by hydrogen by assuming $V_{0e} = V_{0h} = V_0$. Using this value of V_0, the band gaps corresponding to Si wires of different diameters terminated by hydrogen were estimated and compared with the results of first principle calculations[31] as shown in Figure 4a. Here, we use $\epsilon = 11$, $m_e^* = 0.2m_e$, $m_h^* = 0.5m_e$, and $m_0 = m_e$.[32] A good agreement with the first-principle calculation can be seen. It is worth pointing out here that the band gap is found to be nearly the same as long as the sum $V_{0e} + V_{0h}$ is the same, even when $V_{0e} \neq V_{0h}$. This implies that the color of the luminescence is sensitive to the surrounding matrix but is not sensitive to whether it is n-type or p-type, whereas the efficiency is very sensitive to it.

Now, we correlate the band gap of a porous silicon with the ratio Si−O/Si−H bond concentrations. The value of $E_g^{(m)}$ used for polysilane is 4.69 eV,[30] whereas it is 11.5 eV for SiO_2.[33] As the bond ratio of Si−O/Si−H is varied, $E_g^{(m)}$ was obtained from the relation

$$E_g^{(m)} = \text{conc.(Si−O)} \times E_g^{(m)}(SiO_2) + \text{conc.(Si−H)} \times E_g^{(m)}(\text{polysilane})$$

The band gap was estimated for different bond ratios and compared with the experimental results[6] as shown in Figure 4b. The diameter of the porous silicon is assumed to be 2.5 nm, as it is not quoted in ref 6. It may be noted that as the bond ratio of Si−O/Si−H increases the confinement potential and thus also the band gap increases. This example shows clearly that the band gap of nanoparticles of a given diameter can be tuned by changing the surrounding matrix and hence, the color of luminescence can also be changed by changing the surrounding matrix. An experimental evidence has been provided very recently by Passaseo et al.[7] who showed that the wavelength of luminescence of InGaAs quantum dots can be tuned by controlling the barrier surrounding the quantum dots.

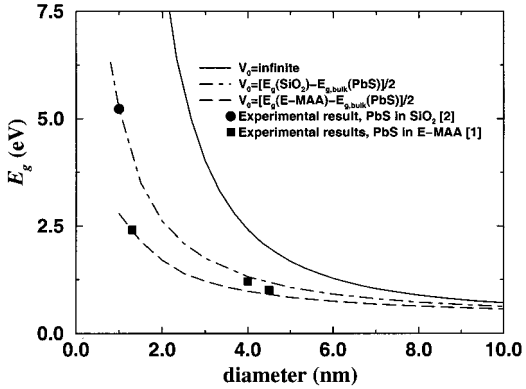

Figure 5. Comparison of the experimental band gap of PbS nanocrystals embedded in SiO_2 matrix[2] and in E-MAA[1] with the finite-depth square-well model. The values of V_0 used for the calculation are 5.545 and 1.75 eV for PbS nanocrystals in SiO_2 matrix and in E-MAA, respectively. The other parameters are $m_e^* = m_h^* = 0.085m_e$ and $m_0 = m_e$.[1] The band gap calculated for the infinite potential is shown by the solid line.

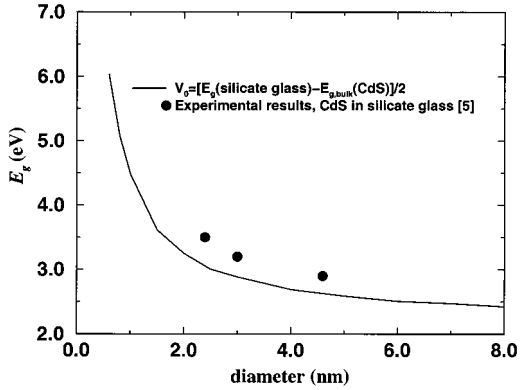

Figure 6. Comparison of the experimental band gap of CdS nanoparticles embedded in silicate glass[5] is compared with finite-depth square-well model. The material parameters used for the calculation are $V_0 = 2.3$ eV, $m_e^* = 0.18m_e$, $m_h^* = 0.53m_e$, and $m_0 = m_e$.[24]

(2) PbS Nanoparticles Embedded within SiO_2 and E-MAA. To test further the validity of the formulation quantitatively, we compared the experimental data of PbS and CdS with different surrounding matrices. The band gap of E-MAA as estimated from the optical absorption data[1] is ≈3.91 eV, which implies that the height of the potential in case of PbS in E-MAA is ≈1.75 eV, whereas $V_0 = 5.545$ eV for PbS nanocrystals in SiO_2. By using respective V_0 values, $m_e^* = m_h^* = 0.085m_e$, $m_0 = m_e$, and $\epsilon = 17.2$,[1] we estimated the change in band gap of PbS nanoparticles embedded in SiO_2 and E-MAA and compared it with the experimental data[1,2] as shown in Figure 5. As expected, the band gap energies are found to be different if the same material is embedded in different matrices and are in excellent agreement with the experimental data.

(3) CdS Nanoparticles Embedded within Silicate Glass. The band gap of sodium silicate glass[34] is ≈7.0 eV, which implies that the height of the potential is 2.3 eV for CdS in silicate glass. In this context it is worth pointing out that the photoionization experiment predicts the height of the potential barrier for electrons in the CdS microcrystals embedded in glass to be in the range 2.3−2.5 eV.[35] Taking $m_e^* = 0.18m_e$, $m_h^* = 0.53m_e$, $m_0 = m_e$, $V_0 = 2.3$ eV, and $\epsilon = 5.5$,[24] we estimated the band gap of CdS nanoparticles embedded in silicate glass and compared it with the experimental data of Ekimov et al.[5] in Figure 6 for the further verification of the finite depth square-well model. The experimental data is found to be in good agreement with this model.

In conclusion, most of the optical properties of semiconducting nanoparticles can be understood by using the square-well potential of finite depth. Though the model is simple, the agreement with experiment is excellent. The Coulomb energy estimated using this model is also found to be in agreement with the pseudopotential calculation. The model predicts that the band gap of a semiconducting material can be tuned, apart from nanocrystal size, by changing the surrounding matrix. As to technological applications, the color of luminescence can be tuned and a higher efficiency of PECS can be achieved by changing the surrounding matrix. Another important outcome of the work is the better approximated ground-state wave function in 1D [eq 11a] which can now be used for the calculation of electron−electron and electron−impurity interactions in addition to the calculation of the energy levels.

Acknowledgment. This work has been supported by the German National Science Foundation (DFG) in the framework of the Special Research Program on "Nanoparticles from the gas phase: formation, structure and properties" (SFB 445).

References

(1) Wang, Y.; Suna, A.; Mahler, W.; Kasowski, R. *J. Chem. Phys.* **1987**, *87*, 7315.
(2) Thielsch, R.; Bohme, T.; Reiche, R.; Schlafer, D.; Bauer, H.-D.; Bottcher, H. *Nanostruct. Mater.* **1988**, *10*, 131.
(3) Wang, Y.; Herron, N. *Phys. Rev. B* **1990**, *42*, 7253.
(4) Vossmeyer, T.; Katsikas, L.; Giersig, M.; Popovic, I. G.; Diesner, K.; Chemseddine, A.; Eychmuller, A.; Weller, H. *J. Phys. Chem.* **1994**, *98*, 7665.
(5) Ekimov, A. I.; Efros, Al. L.; Onuschenko, A. A. *Solid State Commun.* **1985**, *56*, 921.
(6) Tsybeskov, L.; Fauchet, P. M. *Appl. Phys. Lett.* **1994**, *64*, 1985.
(7) Passaseo, A.; Maruccio, G.; Vittorio, M. De; Rinaldi, R.; Cingolani, R.; Lomascolo, M. *Appl. Phys. Lett.* **2001**, *78*, 1382.
(8) Bube, H. R. *Photoelectronic properties of semiconductors*; Cambridge University Press: New York, 1992.
(9) Moser, J.; Grätzel, M. *Helv. Chim. Acta* **1982**, *65* 1436.
(10) Yu, G.; Gao, J.; Hummelen, J. C.; Wudl, F.; Heeger, A. J. *Science* **1995**, *270*, 1789.
(11) Colvin, V. L.; Schlamp, M. C.; Alivisatos, A. P. *Nature* **1994**, *370*, 354.
(12) Wang Y.; Herron, N. *J. Chem. Phys.* **1991**, *95*, 525.
(13) Mahamuni, S.; Khosravi, A. A.; Kundu, M.; Kshirsagar, A.; Bedekar, A.; Avasare, D. B.; Singh, P.; Kulkarni, S. K. *J. Appl. Phys.* **1993**, *73*, 5237.
(14) Efros, Al. L.; Efros, A. L. *Sov. Phys. Semiconduct.* **1982**, *16*, 772.
(15) Brus, L. E. *J. Chem. Phys.* **1983**, *79*, 5566.
(16) Weller, H.; Schmidt, H. M.; Koch, U.; Fojtik, A.; Baral, S.; Henglein, A.; Kunath, W.; Weiss, K.; Dieman, E. *Chem. Phys. Lett.* **1986**, *124*, 557.
(17) Rajh, T.; Peterson, M. W.; Turner J. A.; Nozik, A. J. *J. Electroanal. Chem.* **1987**, *228*, 55.
(18) Kayanuma, Y.; Momiji, H. *Phys. Rev. B* **1990**, *41*, 10261.

(19) Tran Thoai, D. B.; Hu Y. Z.; Koch, S. W. *Phys. Rev. B* **1990**, *42*, 11261.
(20) Nosaka, Y.*J. Phys. Chem.* **1991**, *95*, 5054.
(21) Horiguchi, S. *Physica B* **1996**, *227*, 336.
(22) Gold, A.; Ghazali, A. *Phys. Rev. B* **1990**, *41*, 7626.
(23) Lai, W. I.; Das Sarma, S. *Phys. Rev. B* **1986**, *33*, 8874.
(24) Lippens P. E.; Lannoo, M. *Phys. Rev. B* **1989**, *39*, 10935.
(25) Abramowitz, M.; Stegun, I. A. *Handbook of Mathematical Functions*; Dover: New York, 1965; p 360.
(26) Brus, L. E. *J. Chem. Phys.* **1984**, *80*, 4403.
(27) Franceschetti, A.; Zunger, A. *Phys. Rev. Lett.* **1997**, *78*, 915.
(28) Báyani, L.; Gilliot, P.; Hu, Y. Z.; Koch, S. W. *Phys. Rev. B* **1992**, *45*, 14136.
(29) Rabani, E.; Hetényi, B.; Berne, B. J.; Brus, L. E. *J. Chem. Phys.* **1999**, *110*, 5355.
(30) Read, A. J.; Needs, R. J.; Nash, K. J.; Canham, L. T.; Calcott, A. J.; Qteish, A. *Phys. Rev. Lett.* **1992**, *69*, 1232.
(31) Ohno, T.; Shiraishi, K.; Ogawa, T. *Phys. Rev. Lett.* **1992**, *69*, 2400.
(32) Delley, B.; Steigmeir, E. F. *Appl. Phys. Lett.* **1995**, *67*, 2370.
(33) Evrard, R.; Trukhin, A. N. *Phys. Rev. B* **1982**, *25*, 4102.
(34) Trukhin, A. N.; Tolstoi, M. N.; Glebob, L. B.; Savelev, V. L. *Phys. Status Solidi B* **1980**, *99*, 155.
(35) Grabovskis, V. Ya.; Dzenis, Ya. Ya.; Ekimov, A. I.; Kudryavstev, I. A.; Tolstoi, M. N.; Rogulis, U. T. *Sov. Phys. Solid State* **1989**, *31*, 149.

NL0100318